Fusion Engineering and Design 128, 2018

https://doi.org/10.1016/j.fusengdes.2018.01.025

Preliminary results of a new MIMO plasma shape controller for EAST

Y. Guo [a], B. J. Xiao [a, b], Y. H. Wang [c], L. Liu [a, Ŧ], Y. Huang [a], Q. P. Yuan [a], A. Pironti [d], R. Albanese [d], R. Ambrosino [d], F. Yang [e], Q. L. Qiu [a], G. Calabrò [f], F. Crisanti [f]

[a] Institute of Plasma Physics, Chinese Academy of Science, Hefei, 230031, China

[b] School of Nuclear Science and Technology, University of Science and Technology of China, Hefei, 230026, China

[c] CAS Key Laboratory of Basic Plasma Physics and Department of Modern Physics, University of Science and Technology of China, Hefei 230026, China

[d] CREATE - Università degli Studi di Napoli Federico II and Università di Napoli Parthenope - Via Claudio 21, 80125 Napoli

[e] Department of Computer Science, Anhui Medical University, Hefei, China

[f] ENEA Unità Tecnica Fusione, C.R. Frascati, Via E. Fermi 45, 00044 Frascati, Roma, Italy

[Ŧ] corresponding author E-mail: liulei@ipp.ac.cn

Preliminary results of a new MIMO plasma shape controller for EAST

Y. Guo [a], B. J. Xiao [a, b], Y. H. Wang [c] , L. Liu [a, Ł], Y. Huang [a], Q. P. Yuan [a], A. Pironti [d], R. Albanese [d], R. Ambrosino [d], F. Yang [e], Q. L. Qiu [a], G. Calabrò [f], F. Crisanti [f]

[a] Institute of Plasma Physics, Chinese Academy of Science, Hefei, 230031, China

[b] School of Nuclear Science and Technology, University of Science and Technology of China, Hefei, 230026, China

[c] CAS Key Laboratory of Basic Plasma Physics and Department of Modern Physics, University of Science and Technology of China, Hefei 230026, China

[d] CREATE - Università degli Studi di Napoli Federico II and Università di Napoli Parthenope - Via Claudio 21, 80125 Napoli

[e] Department of Computer Science, Anhui Medical University, Hefei, China

[f] ENEA Unità Tecnica Fusione, C.R. Frascati, Via E. Fermi 45, 00044 Frascati, Roma, Italy

[Ł] corresponding author E-mail: liulei@ipp.ac.cn

ABSTRACT. The efficient and safe operation of large fusion devices relies on plasma configuration inside the vacuum chamber. Due to EAST PF coils distribution, it is difficult to physical decouple plasma control parameters and poloidal field (PF) coils current. In this paper we present a MIMO decoupling controller aimed to overcome the intrinsic limitations of simpler SISO controller, this new controller has been validated by means of the Tokamak Simulation Code (TSC) and implemented on the EAST tokamak. Preliminary results show the potential of this approach for the EAST plasma shape control systems.

PACS numbers: 52.55.Fa, 52.65.-y, 52.50.Nr

Keyword: multiple-input multiple-output, plasma shape control, EAST, TSC

1. Introduction

The efficient and safe operation of large fusion devices relies on plasma configuration inside the vacuum chamber [1]. During the discharge, we should carefully control the plasma shape, to make the plasma maintain adequate clearance from the chamber wall to avoid high density of power and particle deposition, but keep close to the passive plate to ensure adequate passive stabilization. The plasma shape around the antenna should be controlled for

efficient radio frequency (RF) heating. For the advanced plasma configuration, such as snowflake configuration and X-divertor configuration, the magnetic field around the strike point should be optimized to reduce heat deposition. The controlled parameters should be selected according to the experiment purposes.

Experimental Advanced Superconducting Tokamak (EAST) is a D-shaped cross section tokamak with 12 independent poloidal field (PF) coils (PF7 and PF9, PF8 and PF10 are connected together respectively). In present EAST experiment, A Single-Input Single-Output (SISO) method has been used to control the plasma shape, with this approach each PF coils is associated to one controlled variable. The controlled variables should be carefully selected to make sure that each of them strongly rely on one PF coil and be weakly affected by the other 11 coils. The distribution of the PF coils makes that only control points along several special segments could be selected for SISO control, so as it was not possible to select the controlled variables in such a way to achieve specific goals. A Multi-Input Multi-Output (MIMO) approach, which decouples the relationship between control parameters and PF coils, is proposed to solve this problem.

In 2016 EAST campaign, MIMO method has been used for lower singular null (LSN) configuration control. In this paper, the preliminary results are shown. In section 2, the MIMO control scheme for EAST LSN configuration is briefly introduced. Similar control logic model has been implemented in the tokamak simulation code (TSC) [2, 3]. The simulation results are given in section 3. In section 4, we use this method for the LSN configuration control in EAST, and the preliminary results are presented. Finally, the conclusion is given in section 5.

2. **Isoflux control scheme for EAST LSN configuration**

In EAST the major and minor radius are 1.8m, and 0.4m, respectively, its flexibility allows for a large number of plasma configuration, with elongation ranging in the interval 1.5-2, and triangularity ranging in the interval 0.3-0.6. There are 14 PF coils to shape the plasma (PF7 and PF9, PF8 and PF10 are connected together respectively, so as the number of independent circuit is 12) and 2 inner coils (IC1 and IC2) for fast vertical stabilization. In figure 1 the coils are shown as red box, whereas their positions are given in table 1. The designed maximum allowed current in each PF coils is 14 KA/turn. Differently from other tokamaks, such as NSTX or DIII-D, the PF coils number is small (only 12 independent circuits), it follows that the decoupling of the controlled variables is difficult and constrained by the PF coils distribution. Controlled variables are defined along control segments, when SISO controllers are used, each PF coil is assigned to a segment, and the poloidal flux in a target point on the segment is driven to the plasma boundary flux.

In EAST, as it is shown in figure 2, the current isoflux control scheme [4] is divided into 3 parts, plasma current (Ip) control, vertical position (Zp) control and shape control.. The vertical position Zp, estimated by the available magnetic measurements, is controlled by two loops, namely a slow Z control loop, achieved by means of the PF11 – PF14 coils, and a filtered fast Z control loop, achieved by means of the the inner coils (IC). The role of Zp control is to keep the plasma vertical position and control the vertical displacement event (VDE). Shape control is the core part of the isoflux control scheme. The controlled variables are calculated by PEFIT [5, 6]. The relationship between the controlled parameters and the 12

independent PF coils currents is represented by a suitable matrix (M-matrix). In this scheme, the difference between the SISO and the MIMO controllers are in the M-matrix. Indeed, in the SISO controller the M-matrix is a sparse matrix, whereas this does not happen for the MIMO controller. The current flowing in the PF circuits are the sum of a feed-forward term and the feedback terms generated by the three separate controllers.

For EAST LSN configuration control, the plasma target shape is shown as a black line in figure 3, while the control segments are shown in magenta. The control points are the intersection between the plasma boundary and the control segments. It follows that, for LSN configurations, it is necessary to control the poloidal flux at the 8 control points, and the radial and vertical magnetic field at the target X-point location. Assuming that the plasma current variation due to the feedback PF current is small, we could roughly approximate the poloidal flux variation at control points and the magnetic field variation at the target X point as

$$\vec{\vec{G}} \cdot d\vec{I}_{PF} = \begin{bmatrix} G_{i,j}^{\psi} \\ G_{X,j}^{Br} \\ G_{X,j}^{Bz} \end{bmatrix} \cdot d\vec{I}_{PF} = \begin{bmatrix} d\psi_i \\ B_R \\ B_Z \end{bmatrix} = \vec{e} \qquad (1)$$

$G_{i,j}^{\psi}$ is the mutual inductance between the j-th PF currents (j=1,…,12) and the i-th control point (i=1,…,8), while the radial and vertical magnetic field at the X point is $\sum_{j=1}^{12} G_{X,j}^{Br} \cdot I_{PF}^{j}$ and $\sum_{j=1}^{12} G_{X,j}^{Bz} \cdot I_{PF}^{j}$, respectively. $d\psi_i = \psi_i - \psi_{bdry} (i = 1,...,8)$ represent the poloidal flux error to the plasma boundary flux ψ_{bdry}. B_R and B_Z are the radial and vertical magnetic field at the target X points, which should be zero during the discharge. This equation is similar to the equation (6) in reference [7].

Actually, the feedback PF coil current driven by the shape controller will cause a plasma current variation. Nevertheless, since the plasma current is a controlled variable the overall effect of the closed loop controller will make this variation small, and will drive the plasma to the target configuration. A Similar approach has been used for the control of diverted plasmas in [8].

In the current PCS control scheme shown in figure 2, the M-matrix could be equal to $\vec{\vec{G}}^{-1}$. Nevertheless, considering the necessity of having a trade-off between control effort (i.e. amplitude of the feedback PF coil currents) and accuracy on the controlled variables, we resort to a singular value decomposition approach. Let $\vec{\vec{G}} = \vec{\vec{U}} \cdot \vec{\vec{\Sigma}} \cdot \vec{\vec{V}}^T$ be the singular value decomposition in economy form of the G matrix,, i.e. $\vec{\vec{U}}$ is a 14*12 unitary matrix, $\vec{\vec{V}}$ is a 12*12 unitary matrix, and $\vec{\vec{\Sigma}}$ is a 12*12 diagonal matrix, i.e. $\vec{\vec{\Sigma}} = diag(\sigma_1,...,\sigma_{12}).\vec{\vec{U}}^T\vec{\vec{U}} = I_{12}$, and $\vec{\vec{V}}^T\vec{\vec{V}} = I_{12}$ [9].

The PF coils are superconductor, and they have prescribed limitations in terms of maximum applied voltages and maximum flowing currents. As a consequence a large control effort can trigger the PF coils protections, giving rise to a possible plasma disruption. As a results, truncation of the SVD is achieved to balance between the control effort and the control accuracy. The M-matrix is rewrite as $\vec{\vec{V}} \cdot \vec{\vec{\Sigma}}_{new}^{-1} \cdot \vec{U}^T$.

3. Results of TSC simulation

The control model, which is similar to EAST current iso-flux control scheme, has been built in TSC code. Following the designed experiments, the simulation begins with RZIp control from 0.4 s (initial equilibrium) to 2.7 s, which only control the plasma current, and the radial & vertical position of plasma current center. From 2.7 s to 6.7 s (when ramp down), the iso-flux control scheme is switched on. Besides the plasma current and vertical plasma current center, the poloidal flux of 8 control points and Br & Bz at the target X point are controlled by MIMO method. The control points and target X position are listed in table 2, which are used in shot 68988.

With the control points and target X point, $\vec{\vec{G}}$ matrix in equation 1 is easy to calculate, and the matrix of $\vec{\vec{U}}$, $\vec{\vec{\Sigma}}$ and $\vec{\vec{V}}$ are decided by SVD method. Different truncation of $\vec{\vec{\Sigma}}$ are tested by TSC simulation, and find that it is enough to keep the first 9 eigenvalue for desired control results. So, the M matrix is $\vec{\vec{V}} \cdot \vec{\vec{\Sigma}}_{new}^{-1} \cdot \vec{U}^T$, and $\vec{\vec{\Sigma}}_{new} = diag(\sigma_1,...,\sigma_9,0,0,0)$. The control results of the 8 control points and Br & Bz at the target X point are shown as figure 4. With the MIMO control, the plasma configuration is steady after 3.5 sec, which the control errors is smaller than 3.0e-3 Wb at control point and Br & Bz smaller than 1.0e-3 T at the target X point, and the position deviation is in the scale of 1 cm.

Figure 5 gives the 2D flux distribution calculated by TSC code at at 2.6 s, 3.0 s, 3.5 s, 4.0 s, 5.0 s and 6.7 s. The control points and target X point are signed as magenta points, while the plasma boundary is shown as black line. At 2.6 s, the rough target plasma LSN configuration is formed due to careful design of PF feed-forward current wave. The control points are around the plasma boundary. With MIMO control, the plasma shape is corrected to the target configuration. All control points are moved to plasma boundary, and keep the configuration to the end of simulation (6.7 s).

For comparison, a TSC simulation without MIMO control has been done, shown as figure 6. In this case, we only control plasma current and vertical position after 2.7 s. The plasma shape is mainly decided by feed-forward current wave, and plasma shape deviate from the target configuration, which proves that the designed MIMO control method is valid for the plasma shape control.

4. Results of LSN configuration control

In 2016 EAST campaign, this control scheme is used for LSN configuration discharge. Shot 68988 is one typical discharge. For this shot, the feed-forward PF current waves and the target plasma configuration are same to the TSC simulation. Same to the simulation, this

discharge begins with RZIp control to 2.7 s, and then iso-flux control scheme from 2.7 s to 6.7 s when the plasma current ramp-down. The control points and target X position are listed in table 2, and the M matrix is same to the matrix used in TSC simulation. Recently, TSC could not be used to optimize the PID parameters. So, we should test the PID parameters in experiment.

Figure 7 shows the poloidal flux errors at 8 control points and Br & Bz at target X point. The poloidal flux error at 8 control points is smaller than 6.0e-3 Wb after 3 s. The Br of target X point is smaller than 1.0e-3 T from 3 s to 6.7 s, while Bz is nearly in the scale of 2e-3 T. The accuracy of control effect is close to TSC simulation. In this experiment, GI values (integral gains) for all control parameters are increased from 4.9 s for PID parameters test, which may be responsible to the oscillation since 5 s.

The actual PF current waves (red line) are shown in figure 8. Compared with the feed-forward PF current waves (blue dashed line), the PF currents, especially PF11 – PF14, are corrected dramatically to fix the plasma shape. It proves that the iso-flux control scheme significantly change the PF coils current to move the plasma shape to the target configuration.

In figure 9, the 2D poloidal flux distribution calculated by PEFIT at 2.7 s, 3.0 s, 3.6s, 4.0 s, 4.9s and 6.0 s are given. The plasma boundaries are shown by black line, while the 8 control points and the target X point are signed by red point. At 2.7 s, the initial plasma shape for MIMO control is close to the target due to good feed-forward PF currents. But the control points at seg1, 3, 9 are obviously outsider the plasma boundary. At 3 s, except the first control point, other control points are at the plasma boundary. The plasma shape is controlled to the target configuration from 3.6 s to 4.9 s. From 4.9 s, we increase the GI value for all control parameters, and find the control error begin shake in figure 7. The control errors at the 2^{nd}, 3^{rd}, 4^{th} and 5^{th} control points have little shift, which is shown as the plasma shape shrink at the top shown as 6.0 s flux distribution in figure 9.

5. Conclusion

Due to EAST PF coils distribution, simply SISO control method seems weak for complex plasma shape control. The MIMO control method, which is numerical decoupling the relationship between plasma control parameters and PF coils, has the potential to cope with this problem. For one lower singular null (LSN) configuration, we could reach the target shape by control the poloidal flux at several selected control points and Br & Bz at target X point. This method has been validated by TSC simulation results. In EAST experiment, the preliminary result of shot 68988 has shown that this method could be used for LSN shape control in EAST. The results prove the potential for EAST plasma shape control.

Acknowledge

Numerical computations were performed on the ShenMa High Performance Computing Cluster in Institute of Plasma Physics, Chinese Academy of Sciences.

This work is supported by the National Natural Science Foundation of China under Grant No. 11305216 and No.11375191, the National Magnetic Confinement Fusion Research Program of China under Grant No. 2014GB103000 and 2014GB110003, and External Cooperation Program of BIC, Chinese Academy of Sciences, Grant No. GJHZ201303

REFERENCES

[1] Alessandro B and Angelo C 2005 IEEE Control Systems Magazine 25 44

[2] Jardin S C, Pomphrey N and Delucia J 1986 J. Comput. Phys. 66 481

[3] Yong Guo, et al., Plasma Phys. Control. Fusion 54 (2012) 085022

[4] Q.P. Yuan, et al., Nucl. Fusion 53 (2013) 043009.

[5] X N Yue, et al., Plasma Phys. Control. Fusion 55 (2013) 085016

[6] Yao Huang, et al., Fusion Engineering and Design 112 (2016) 1019–1024

[7] Y. Guo, et al., Fusion Engineering and Design 101 (2015) 101–110

[8] Yong Guo, Bing-Jia Xiao, Lei Liu, et al., Chin. Phys. B Vol. 25, No. 11 (2016) 115201

[9] Ariola. Marco, Alfredo. Pironti, IEEE Control Syst. 25 (2005) 65–75.

Table 1.PF coils geometry and turns in R and Z direction

	R (m)	Z (m)	dR (m)	dZ (m)	N_R	N_Z
PF1	0.62866	0.25132	0.16078	0.45177	7	20
PF2	0.62866	-0.25132	0.16078	0.45177	7	20
PF3	0.62866	0.75396	0.16078	0.45177	7	20
PF4	0.62866	-0.75396	0.16078	0.45177	7	20
PF5	0.62866	1.2566	0.16078	0.45177	7	20
PF6	0.62866	-1.2566	0.16078	0.45177	7	20
PF7	1.07217	1.7537	0.24694	0.09769	11	4
PF8	1.07217	-1.7537	0.24694	0.09769	11	4
PF9	1.13679	1.94092	0.37618	0.27473	17	12
PF10	1.13679	-1.94092	0.37618	0.27473	17	12
PF11	2.94558	1.59073	0.12844	0.21256	6	10
PF12	2.94558	-1.59073	0.12844	0.21256	6	10
PF13	3.2698	0.90419	0.08896	0.17188	4	8
PF14	3.2698	-0.90419	0.08896	0.17188	4	8
IC1	2.3090	0.7425	0.05	0.100	1	2
IC2	2.3090	-0.7425	0.05	0.100	1	2

Table 2. 8 control points and target X point for MIMO validation by TSC code, which are also used in shot 68988 (segment 7 is not included)

	R (m)	Z (m)
Segment 1	2.26014	0.000000
Segment 2	1.52308	0.576644
Segment 3	2.05875	0.558302
Segment 4	1.42715	0.410827
Segment 5	1.70019	0.674475
Segment 6	1.39618	0.000000
Segment 8	1.50012	-0.368266
Segment 9	2.00834	-0.493034
Target X point	1.68836	-0.736757

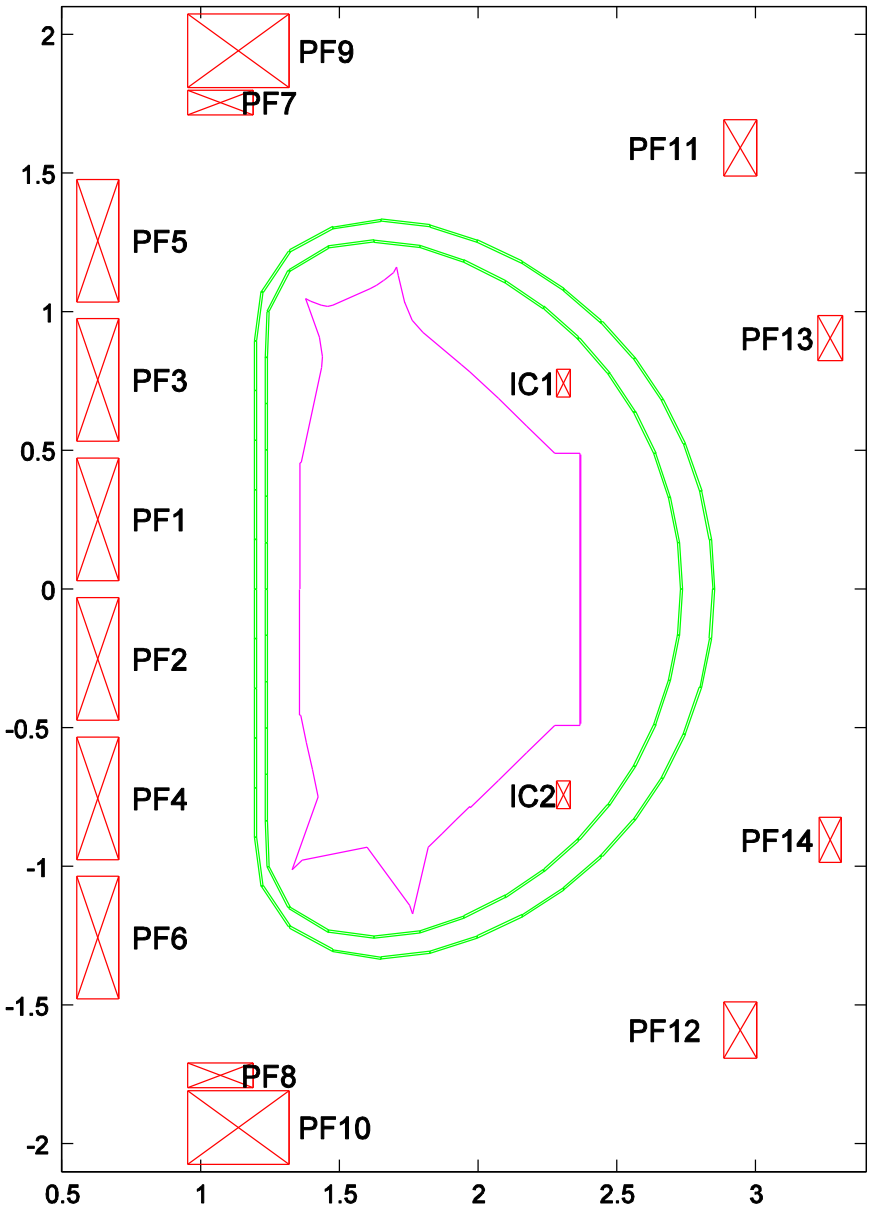

Figure 1. EAST geometry Poloidal Field (PF) locations and sizes are signed by red rectangle boxes, the double layer vacuum vessels are signed by green line.

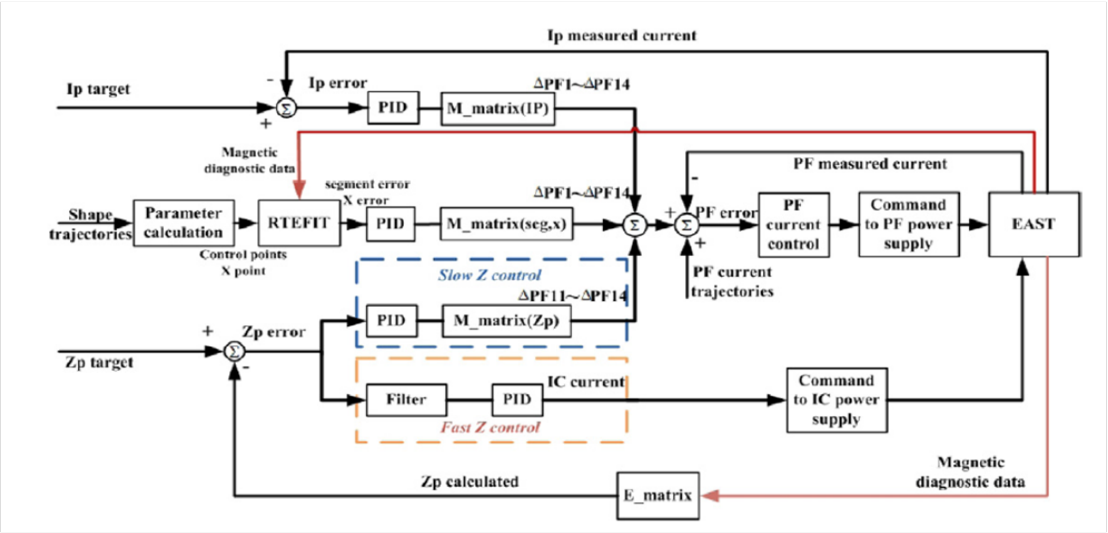

Figure 2 Isoflux control scheme for EAST

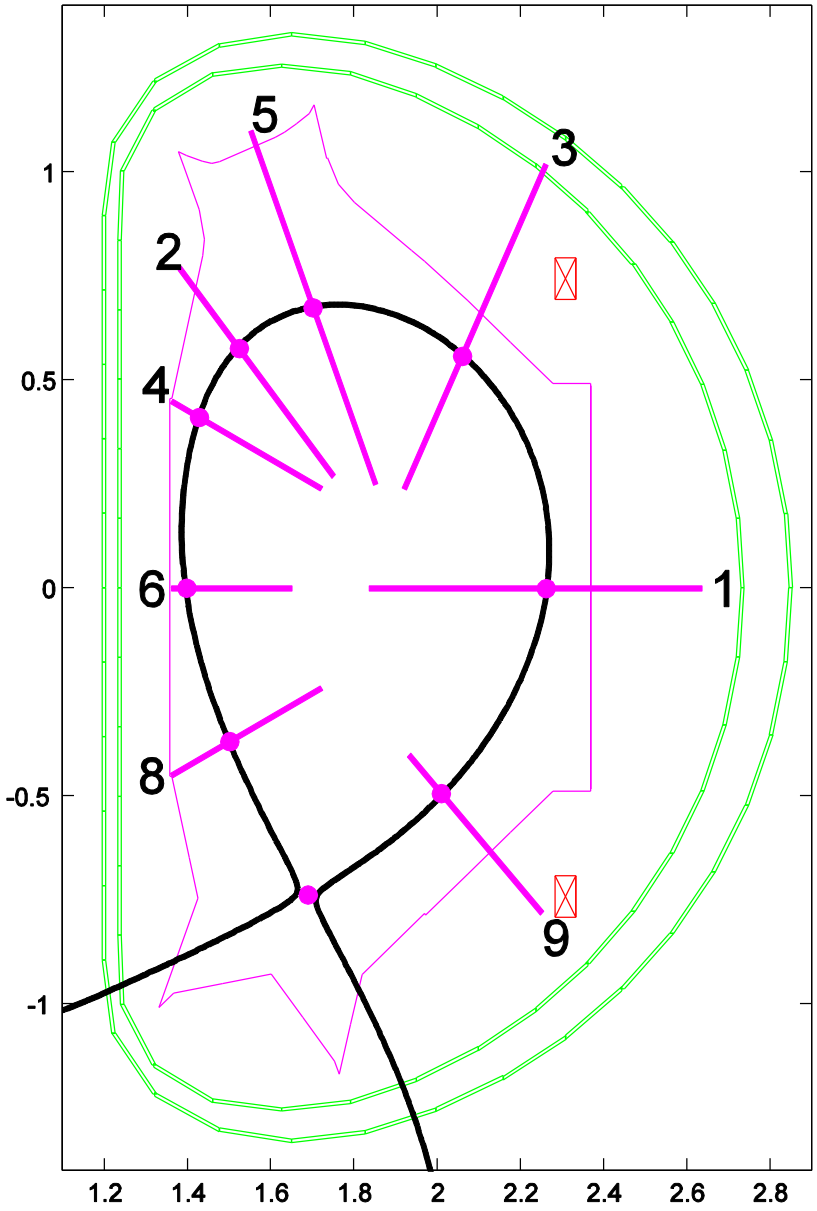

Figure 3 the plasma target shape is shown black line and the control segment line is shown as magenta line (segment 7 is not included in shot 68988)

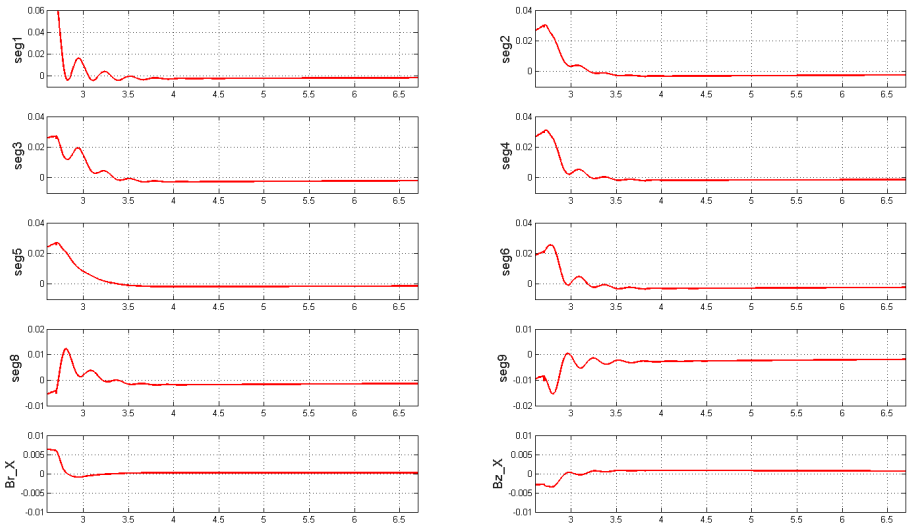

Figure 4 the control errors at 8 control points, while the Br & Bz at the target X point

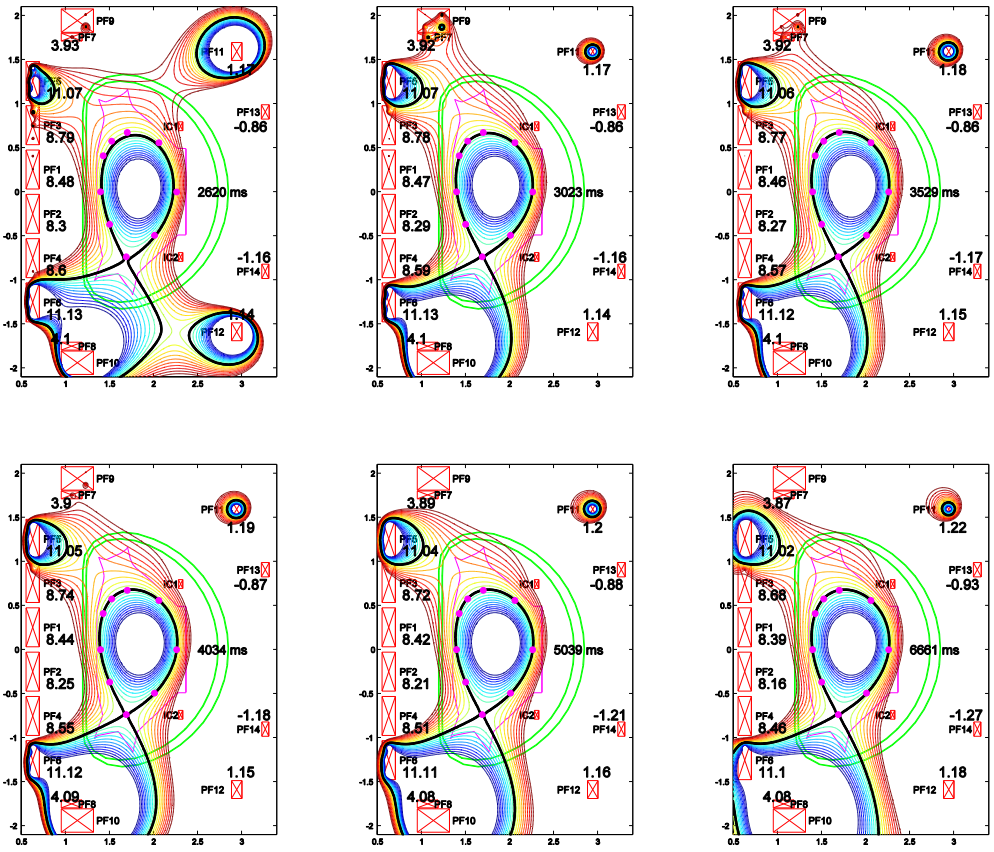

Figure 5 the 2D poloidal flux distribution calculated by TSC simulation at 2.6 s, 3.0 s, 3.5 s, 4.0 s, 5.0 s and 6.7 s with MIMO control

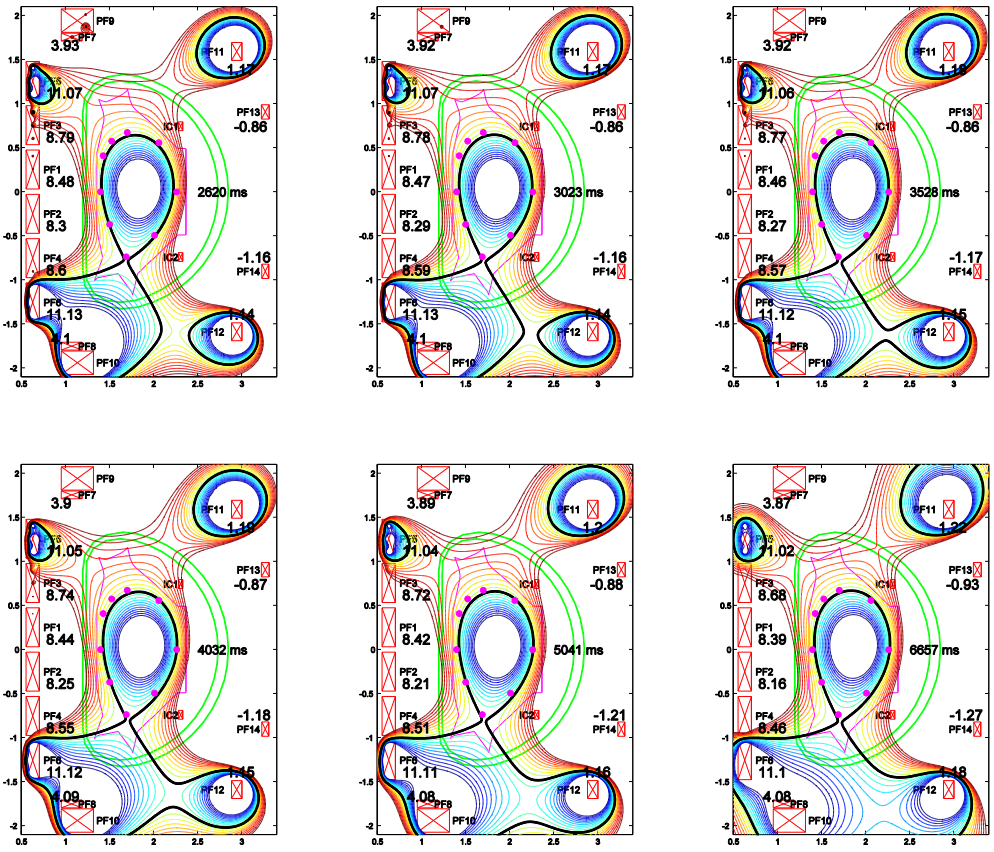

Figure 6 the 2D poloidal flux distribution calculated by TSC simulation at 2.6 s, 3.0 s, 3.5 s, 4.0 s, 5.0 s and 6.7 s without MIMO control

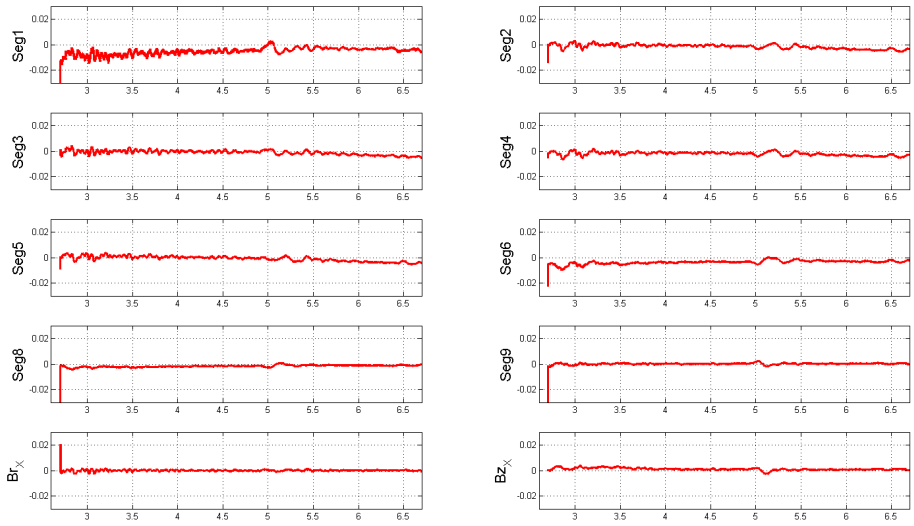

Figure 7 the poloidal flux error at 8 control points and Br & Bz at target X point for shot 68988

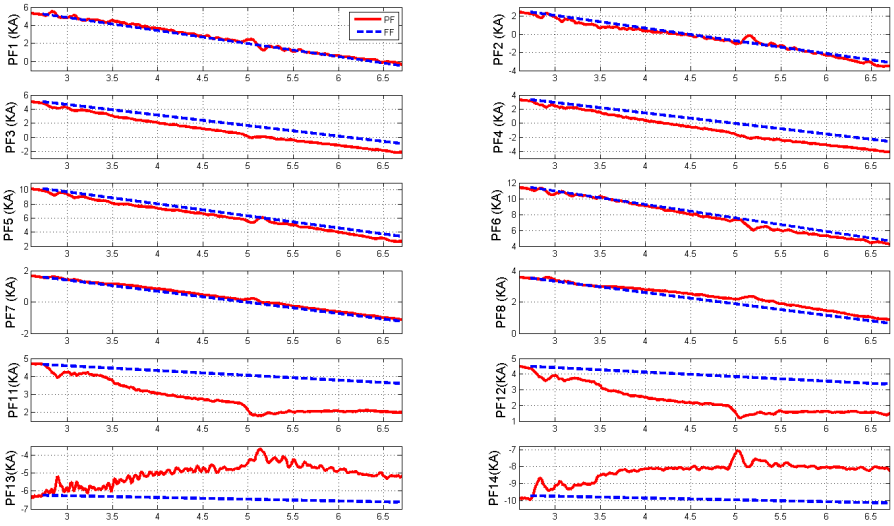

Figure 8 For shot 68988, the actual PF current waves (red line) vs. feed-forward PF current waves (blue dashed line) from 2.7s to 6.7 s when the MIMO control is switched on

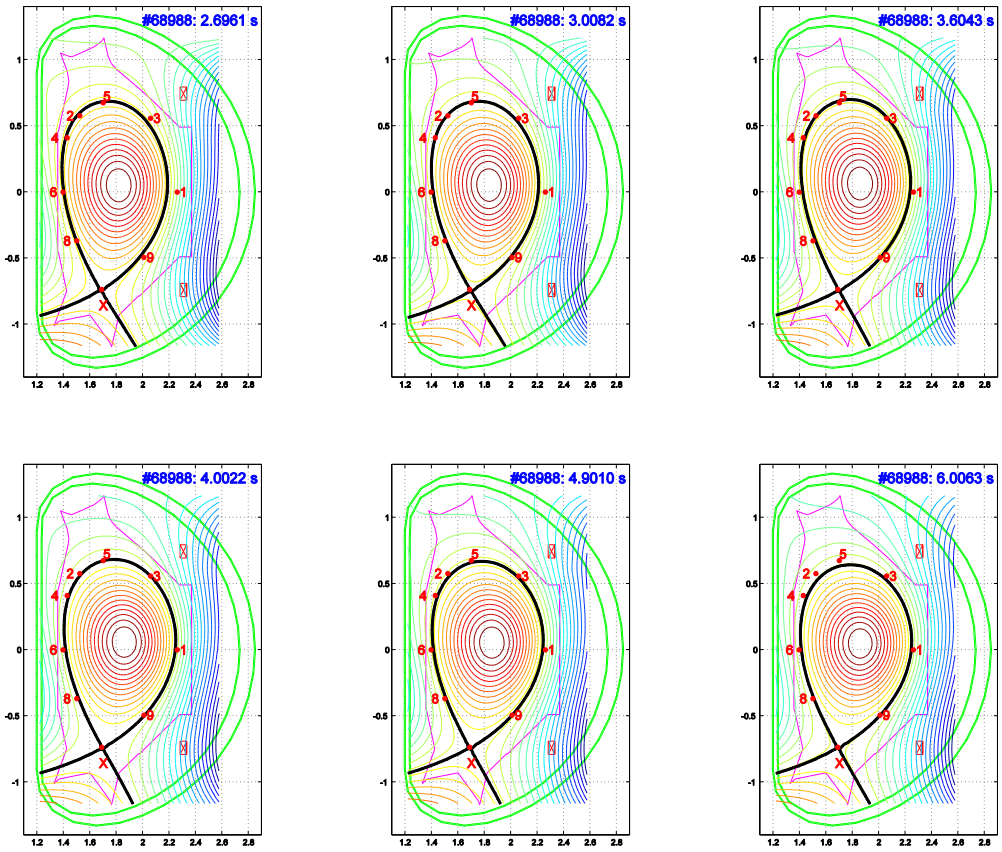

Figure 9 For shot 68988, the 2D poloidal flux distribution calculated by PEFIT at 2.7 s, 3.0 s, 3.6 s, 4.0 s, 4.9 s and 6.0 s